An Intercept and Following Strategy for a Multi-rotor Platform using a Modified Proportional Navigation

Garrett S. Clem, Jay P. Wilhelm
Department of Mechanical Engineering
Ohio University
Athens, Ohio 45701
Email: gc117711@ohio.edu, jwilhel@ohio.edu

David Casbeer, David Grymin, Isaac Weintraub
AFRL RQQA
AFRL
Wright-Patterson Air Force Base, Ohio 45433
Email: david.casbeer@us.af.mil, grymin, isaacweintraub.1@us.af.mil

***Abstract*—Combatant small Unmanned Aerial Vehicles (CUAVs) can easily enter restricted airspace and may be mitigated by counter UAVs. Intercepting and following combatant UAVs in restricted airspace could be achieved with multi-rotor UAVs. A pseudotarget based proportional navigation (PN) guidance algorithm that guides a UAV to intercept and follow a combatant UAV using highly uncertain sensor position information was developed. Simulations were performed to validate the model and develop a ratio of following distance to initial range. Near zero following distance was achieved for a finite range of initial line-of-sight angles.**

***Keywords*—UAV Multi-rotor Fixed Wing Guidance Proportional Navigation Uncertainty**

I. Introduction

Multi-rotor sUAS may be guided to passively track and follow another sUAS. Direction and ranging sensor technology for sUAS currently only provides a highly uncertain position estimation. Proportional navigation guidance has been used by missiles to track targets. PN guidance may be useful for guiding a mutli-rotor sUAS to intercept and follow other sUAS. Intercept and following has applications in autonomous flight formation, swarming, and loyal wingman scenarios as well. The objective was to use a modified PN guidance with uncertain position information to reduce distance to another sUAS.

A. Literature

Tracking a target has been achieved by implementing closed-loop feedback systems, path following guidance, and line-of-sight (LOS) guidance algorithms. Closed-loop position and velocity control of a multi-rotor for following a ground target with intermittent and noisy vision data was achieved in [1]. Following time varying paths and intercepting multiple ground targets was demonstrated in [2] by introducing a heading control law. Modifying an autopilot's low level control may be difficult and may require tuning. Target tracking without modification of a UAVs control system has been accomplished by framing target tracking as a path planning problem. A waypoint generation technique was developed in [3] that satisfied fixed wing forward velocity constraints while maintaining the target in the field-of-view. Sub-optimal placement of waypoints resulted in exaggerated trajectories for fixed wings when tracking an accelerating target. Multi-rotors tracked the target with less error when navigating the waypoints for the same scenario due to the multi-rotors ability to hover. Less exagerated trajectories for tracking a maneuvering target was accomplished for a fixed wing UAV in [4]. An optimal path planning strategy consisting of a Markov Decision Process and cost based state reduction showed less tracking error in comparison to lookup tables and heuristic methods, but took considerably longer to provide a solution [5]. A compromise between path planning and a target tracking control system was found in [6], where a modified pure pursuit line of sight (LOS) guidance chased a target with less tracking error than traditional pure pursuit guidance[6].

Proportional navigation (PN) has been in use since the 1950's [7] and is used primarily to guide missiles to a target by nulling the line-of-sight (LOS) rate [8], [9]. PN guidance has had continued interest and may have new uses such as cooperative defense strategies [10]. The traditional PN guidance law is adequate for commanding a UAV to intercept a target but it would be useful to command the angle in which the UAV would approach the target to prevent unwanted collisions. Ratnoo and Ghose modified the PN guidance gain throughout flight to satisfy a terminal angle constraint [11]. Oza and Padhi discuss how time varying guidance gains result in singularities near the end of the flight and provide an impact-angle-constrained suboptimal model predictive static programming guidance [12]. Optimal impact-angle-constrained guidance algorithms have been developed for 2D [13] and 3D [14] engagements. The impact-angle constrained guidance in literature have additional levels of complexity in comparison to traditional PN guidance and may be more complicated to implement. Achieving a terminal angle constraint can be accomplished without modifying the PN guidance gain or implementing an entirely new guidance model by introducing a pseudotarget into the engagement scenario. The objective was to use a modified PN guidance with uncertain position information to reduce the distance to target, referred to as intercept, and to tail chase the target, referred to as follow.

B. Methods

Interceptor and target kinematics are first presented, followed by the traditional PN guidance law. Next an on-board

sensor that measures the target's position, which has some uncertainty, is modeled. A state machine pseudotarget is introduced that prevents the intercepting UAV from entering the uncertain area while accomplishing the main goal of intercepting and following the target. Simulations were performed to validate the model and to show that the following distance can be predicted from the initial LOS angle, range, and sensor characteristic.

II. Model

A. Intercept Model

Prior to investigating position uncertainty and a state machine pseudotarget, the traditional PN guidance algorithm is presented using Zarchan's notation [7]. Consider a two agent engagement scenario shown in Figure 1 consisting of a target T and an interceptor I. East is the positive X axis and up, or altitude, is the positive Y axis. The interceptor is tasked with intercepting the target whose position at any time is $\vec{X}_T = [x_T y_T]^T$ which is determined from the previous position $\vec{X}'_T$, velocity v_T, and heading β shown in Equation 1. Position of the interceptor $\vec{X}_I$ is updated identically to the target with velocity v_I and heading γ. Headings are measured with respect to the horizontal x axis. dt represents the discrete change in time from one update to the next.

$$\vec{X}_T = \vec{X}'_T + \vec{V}_T dt \tag{1}$$

$$\vec{V}_T = v_T \begin{bmatrix} cos(\beta) \\ sin(\beta) \end{bmatrix} \tag{2}$$

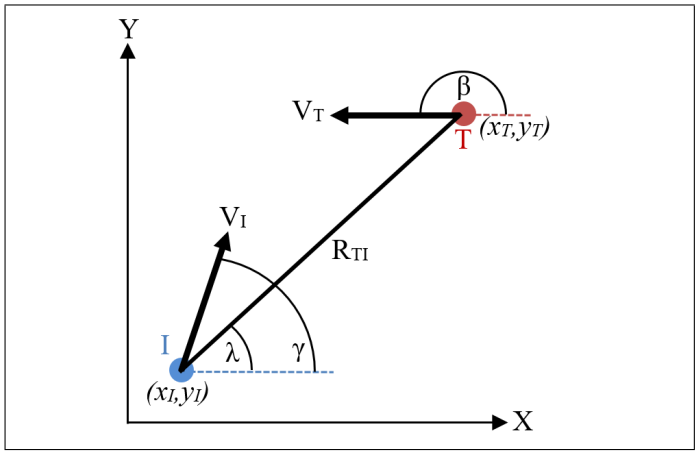

Fig. 1: Interceptor and Target Engagement Scenario (x-East, y-Up)

Heading changes are determined by the PN guidance algorithm operating on the principle of nulling the LOS rate $\dot{\lambda}$ by issuing heading change commands proportional to the LOS rate. For a non zero LOS rate, a heading rate command $\dot{\gamma}$ is issued by multiplying the LOS rate by the fixed guidance gain N.

$$\dot{\gamma} = N\dot{\lambda} \tag{3}$$

Guidance gains of $N < 3$ are generally referred to as conservative while $N > 5$ are referred to as more aggressive [7]. Conservative gains lead to larger turn radii and make for a less maneuverable interceptor. Higher gains result in a more maneuverable vehicle as long as the commanded heading changes are not beyond the vehicles physical capabilities. Multi-rotors are capable of making abrupt heading changes in comparison to fixed wing UAVs and it was assumed a guidance gain of $N = 5$ is not beyond multi-rotor capability. The resulting guidance is expected to return sharp turns and straight line optimal paths when used with the Dubins kinematic model. The LOS angle and rate are calculated in Equations 4 and 5 respectively.

$$\lambda = \tan^{-1}\left(\frac{y_T - y_I}{x_T - x_I}\right) \tag{4}$$

$$\dot{\lambda} = \frac{(x_T - x_I)(V_{Ty} - V_{Iy}) - (y_T - y_I)(V_{Tx} - V_{Ix})}{(x_T - x_I)^2 + (y_T - y_I)^2} \tag{5}$$

Range is the Euclidean distance between the target and the interceptor, shown in Equation 6.

$$R_{TI} = \sqrt{(x_T - x_I)^2 + ((y_T - y_I)^2} \tag{6}$$

The PN guidance law provides a heading rate whereas the model requires a heading. To determine the heading from the heading rate, the second order Runge-Kutta integration technique was used.

PN guidance is effective at reducing the range between the interceptor and the target, however at or near the point of interception a singularity in the LOS rate will occur for head-on interception. The cause of the singularity is due to the near zero range and the change of sign in relative velocities. Solutions around the singularity can be obtained for a linearized proportional navigation [15] but are not of a major concern for traditional missile systems because the mission is complete when the range is near zero. For an intercepting UAV with the intention of following the target, the singularity could call for control efforts beyond the saturation point. Additionally, after the singularity occurs there remains a possibility for the nulled LOS condition to be met even if the interceptor and target are heading away from each other. Figure 2 demonstrates how for head-on intercepts the nulled LOS rate can be satisfied and the interceptor flys away from the target. Figure 3 shows how a singularity can occur near zero range.

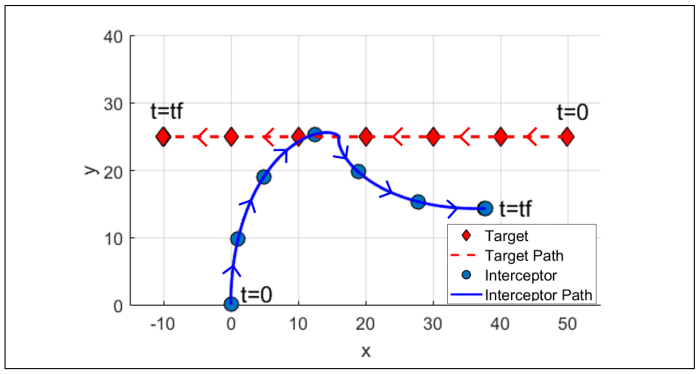

Fig. 2: Failed follow for head on intercept

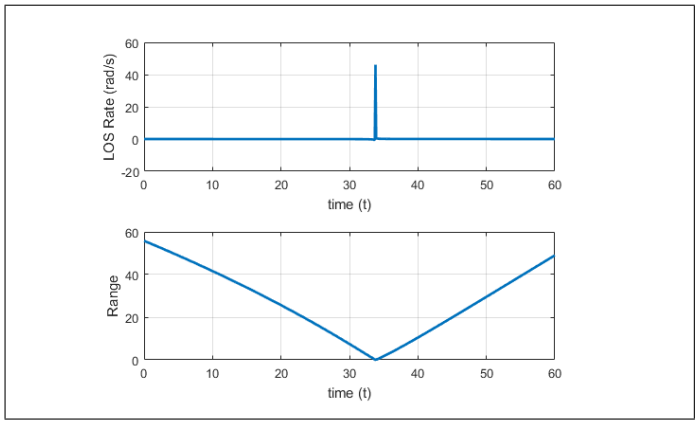

Fig. 3: Failed follow with LOS-rate singularity and range

The interceptor does not fail to intercept and follow the target for a tail-chase scenario shown in Figure 4 and no singularities are present in Figure 5. The tail-chase scenario has the added benefit of placing the interceptor behind the target, allowing for a transition into a follow. The elimination of the singularity and easy transition into a follow make a case for waiting on the target before intercepting it directly, which is the motivation for introducing a pseudotarget into the PN guidance model.

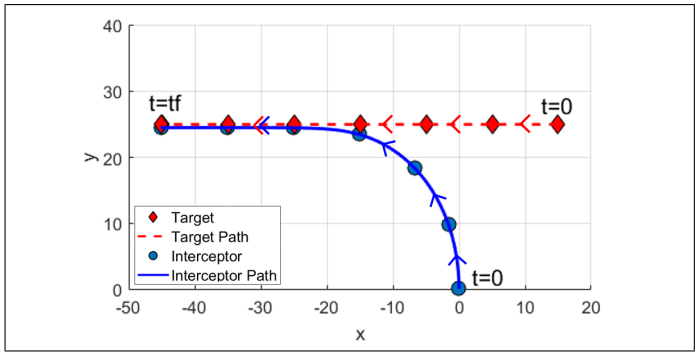

Fig. 4: Successful follow for tail chase intercept

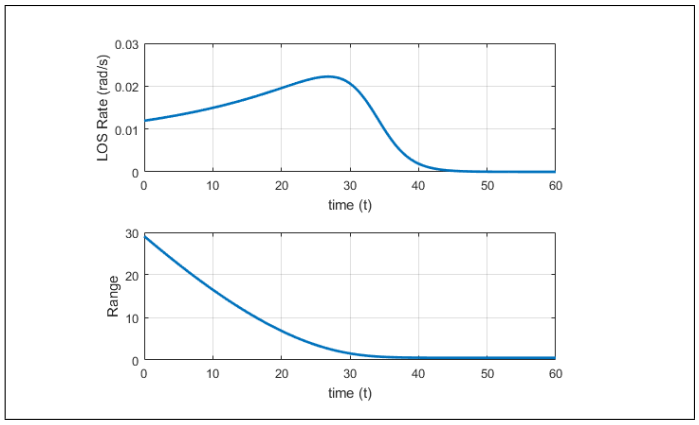

Fig. 5: Successful follow LOS-rate and range

B. Intercept and Follow Model

Measuring the LOS rate and range uncertainties in x and y are assumed to be equal so the actual position of the target is in the space $(x_T \pm r, y_T \pm r)$, where r is the radius of uncertainty. Figure 6 shows a representation of the measurement as a point centered in a circle of radius r. The region inside the circle is the space where the target may actually exist. The interceptor should avoid the inside of the circular region to prevent an unintended collision with the target. The uncertainty decreases linearly as a function of range as shown in Equations 7 and 8.

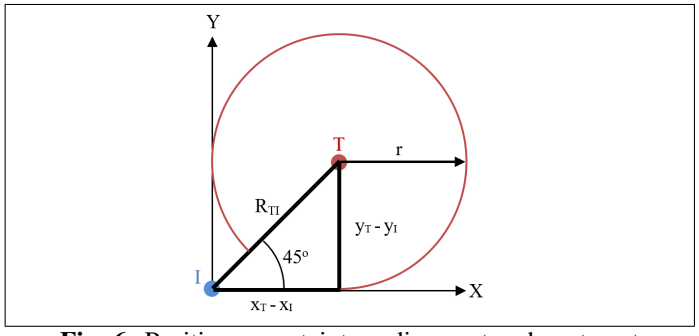

Fig. 6: Position uncertainty radius centered on target

$$r = dr\sqrt{(x_T - x_I)^2 + (y_T - y_I)^2} + b \tag{7}$$

$$b = r_0 - dr\sqrt{(x_{T0} - x_{I0})^2 + (y_{T0} - y_{I0})^2} \tag{8}$$

The radius of position uncertainty r was represented as a function of the range R_{TI}, rate of change dr, and the minimum uncertainty radius b. A pseudotarget was introduced into the engagement scenario which prevents the interceptor from entering the region of uncertainty while maintaining the requirements of intercepting and following the target. The modified guidance was developed to satisfy a small range of scenarios where the target travels at constant heading, altitude, and speed equal to that of the interceptor. The interceptor avoids the region of uncertainty while following and intercepting the target by pursuing a pseudotarget.

The pseudotarget acted as a state machine consisting of $wait$, $intercept$, and $follow$ states shown in Figures 7, 8, and

9 respectively. When the minimum altitude of the uncertainty is below the horizon $y_I - r < 0$ the pseudotarget's state is set to $wait$ and waits at it's current position. Uncertainty decreases as the target approaches the interceptor eventually satisfying the condition $y_I - r > 0$ triggering a change in state from $wait$ to $intercept$. When the $intercept$ state is active the pseudotarget is placed at the minimum uncertainty $y = y_T - r$ with no movement in the x axis, $x = 0$. Placing the pseudotarget at the minimum uncertainty altitude prevents the possibility of an unintended collision with the target. Intercept is intended to reduce the range to the target and get close, but not result in a collision. Once $x_T < x_I$ the problem becomes a tail chase scenario and the risk of collision is non existent. The algorithm is set to the $follow$ state where the pseudotarget is placed on top of the targets estimated position.

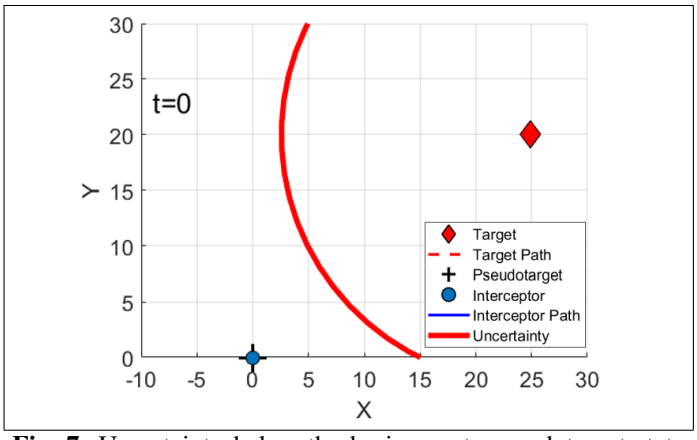

Fig. 7: Uncertainty below the horizon sets pseudotarget state to wait

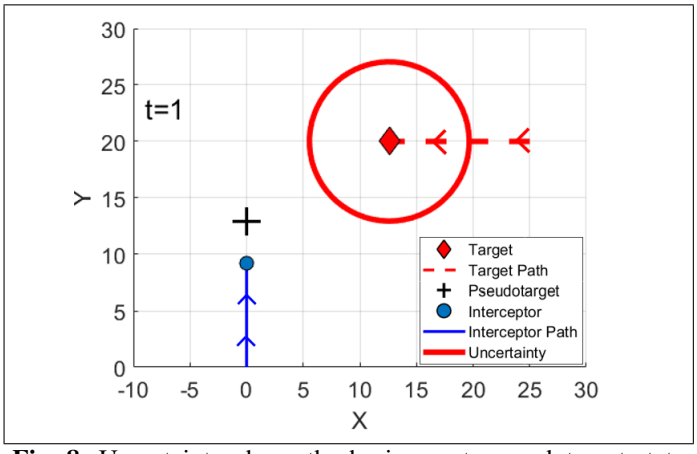

Fig. 8: Uncertainty above the horizon sets pseudotarget state to intercept

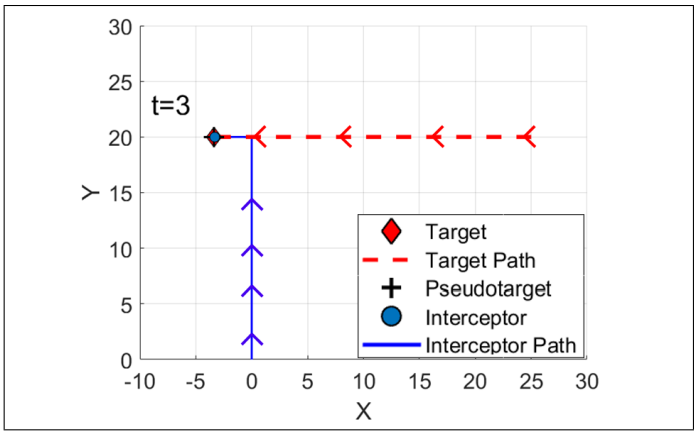

Fig. 9: Target estimate $x_T < 0$ sets pseudotarget state to follow

With the target moving at constant altitude and both vehicles sharing the same velocity, it is expected that the following distance will be near zero if the intercept is active when $x_T \geq y_T$. If the intercept occurs when $x_T < y_T$, the interceptor is at a disadvantage and will fail to close the distance. The sensor was modeled so that the uncertainty circle is above the horizon once the target has crossed the $x = y$ line by calculating an appropriate initial uncertainty r_0. Referring back to Figure 6 a target at a LOS of $45°$, has an altitude of R_{TIy}, and an initial uncertainty radius r_0. Determining the initial radius was done geometrically in Equations 9 and 10 and was set to 0.7 times the initial range.

$$\sin(45°) = \frac{y_T - y_I}{\sqrt{(x_T - x_I)^2 + (y_T - y_I)^2}} \tag{9}$$

$$(y_T - y_I) = \sqrt{(x_T - x_I)^2 + (y_T - y_I)^2}\sin(45°) \tag{10}$$

$$r_0 = 0.7R_{TI} \tag{11}$$

The impact of r_0 on following distance can be seen in Figures 10 and 11. Each Figure shows the results of three target initial conditions along the $x = y$ line. Figure 10 shows a near zero following distance for a r_0 ratio of $0.7R_{TI}$. When $r_0 > 0.7R_{TI}$ the following distance becomes less predictable and is not constant along the target initial conditions on the $x = y$ line as shown in Figure 11.

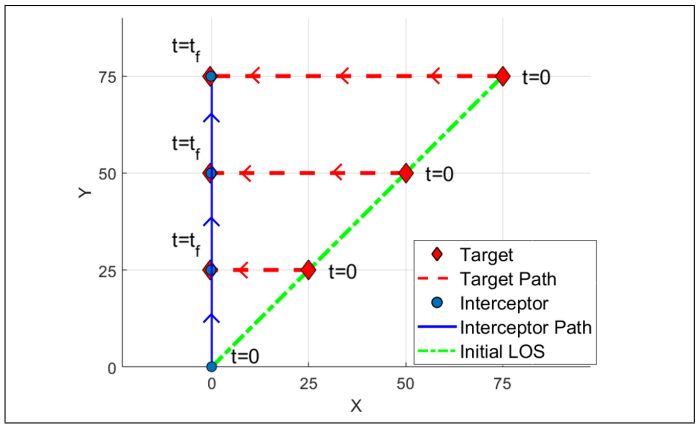

Fig. 10: Initial uncertainty ratio $0.7R_{TI}$ results in consistent following distance

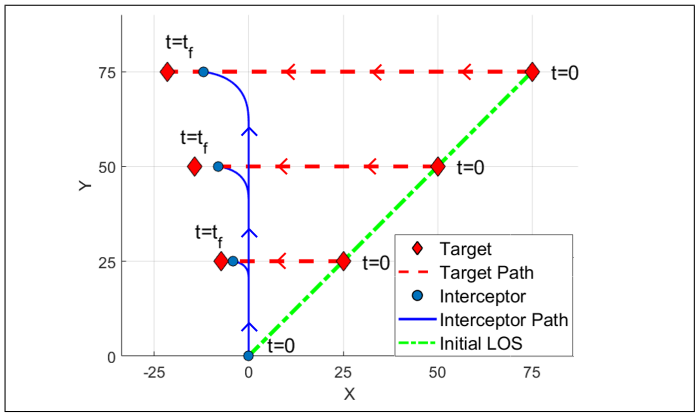

Fig. 11: Initial uncertainty ratio $> 0.7R_{TI}$ results in increasing following distance as initial range increases

The modified pseudotarget PN guidance was given the same initial conditions as shown in Figure 2 and the performance compared. Traditional PN guidance performed well during the tail-chase but failed to follow the target and experienced a LOS singularity for a head-on intercept. The PN guidance with a psuedotarget successfully intercepts and follows the target, Figure 12, with non-singularity LOS rates, shown in Figure 13. Traditional PN out performed the pseudotarget PN guidance for target initial condition $x_T = 15$ which demonstrates that a single guidance algorithm may not be suitable for all cases and a decision on which algorithm to use for a given set of initial conditions should be made. Table I summarizes the performance of the algorithms for the two initial conditions.

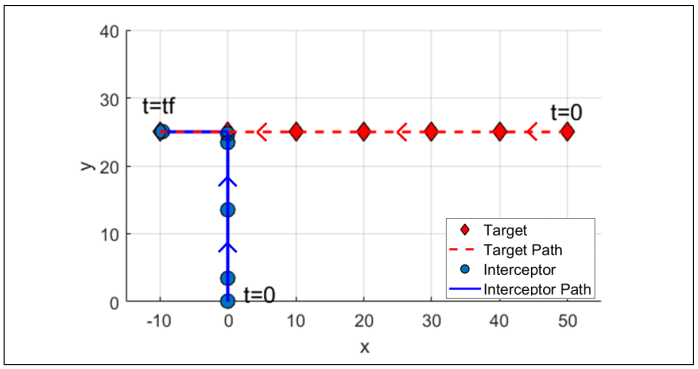

Fig. 12: Tail chase with no singularities, and steady state range $R_{TI} \approx 0$

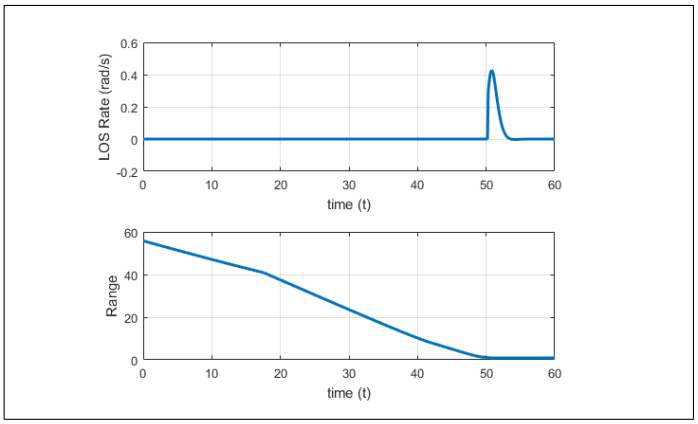

Fig. 13: Tail chase with no singularities, and steady state range $R_{TI} \approx 0$

TABLE I. TRADITIONAL PN AND PSEUDOTARGET PN FOLLOWING DISTANCE AND LOS RATE

	Following Distance	Max LOS Rate (rad/s)
Traditional PN	0.51	0.02
	FAILED	46.07
PN with Pseudotarget	6.51	0.06
	0.88	0.04

III. SIMULATIONS

The pseudotarget state machine PN guidance was validated through MATLAB simulations and a ratio for predicting following distance as a function of initial LOS, range, and sensor characteristic is presented for a non maneuvering target. Initial target conditions of $x = [-100, 100]$ $y = [10, 100]$ in 1 unit increments were evaluated with a constant heading of $\beta = 180°$. Initial uncertainty radius of the target estimate for each scenario was 0.7 times the initial range with rate of change $dr = 1$. Interceptor initial conditions remained constant where the initial position and heading were $(0, 0)$ and $90°$ respectively. Each UAV was given the same velocity so that the speed ratio of the two vehicles was 1:1. When the interceptor's heading $\gamma = \beta$ the simulation was terminated and the final positions of the vehicles recorded. Dividing the following distance by the initial range to the target produces a following distance initial range ratio (FDIR), shown in Equation 12 which can be used to describe the performance of the model.

$$FDIR = \sqrt{\frac{(x_{Tf} - x_{If})^2 + (y_{Tf} - y_{If})^2}{(x_{T0} - x_{I0})^2 + (y_{T0} - y_{I0})^2}} \qquad (12)$$

The unit-less FDIR ratio in the simulation space is shown in the contour plot Figure 14. Each target initial condition corresponds to a FDIR ratio on the plot, ranging from 0 to 1.65. FDIR is constant along each initial LOS which allows for the prediction of following distance based on initial LOS, range, and sensor dr. Initial LOS angles less than $45°$ yield a FDIR ratio of near zero indicating that the following distance was near zero. Increasing LOS angles greater than $45°$ result in progressively higher FDIR ratios indicating an increasing following distance.

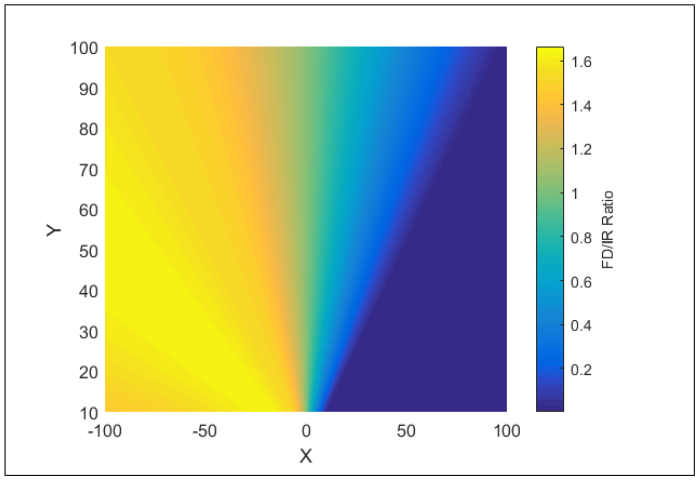

Fig. 14: Following distance to initial range ratio constant along each initial LOS

Representation of the models performance for a range of sensor dr's is shown in Figure 15. Simulations were performed for initial LOS angles ranging from $0°$ to $180°$ and sensors with dr ranging from 0.5 to 1 in $0.5°$ and 0.01 unit increments respectively. Sensors with $dr < 0.5$ would not allow the interceptor to reduce the following distance much farther than the initial range for nearly all LOS angles. Sensors with $dr \geq 1$ the following distance can be reduced to nearly zero for initial LOS angles between 0 and $45°$.

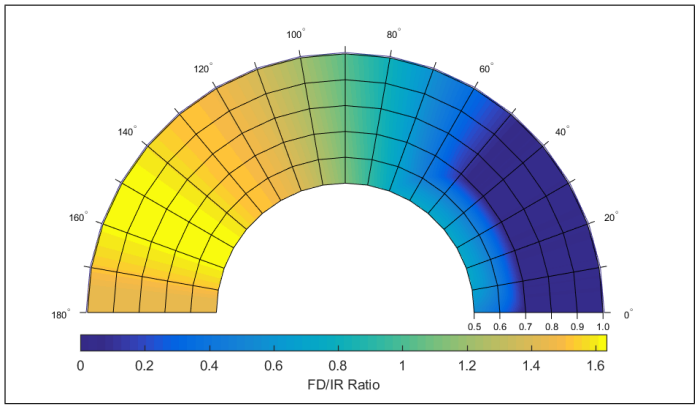

Fig. 15: Following distance to initial range ratio for multiple sensor dr confirm predicted near zero following distance for initial LOS $\leq 45°$

IV. Conclusion

A pseudotarget based proportional navigation (PN) guidance algorithm that guides a UAV to intercept and follow a target UAV using highly uncertain sensor position information was investigated. Simulations were performed to determine the following distance for a finite space. Near zero following distance is achievable for a finite range of initial headings and sensor dr's. Following distance to initial range ratios indicate that the modified guidance performs optimally when the initial LOS angle is less than $45°$ and larger initial sight angles may benefit from other intercept methods. The state machine pseudotarget PN guidance algorithm was specifically designed to intercept and follow an inbound non-maneuvering target for the edge case of $1:1$ speed ratio. Initial results suggest that the proposed guidance is tracks the target with less error compared to traditional PN for head-on intercepts but slightly underperformed in the tail-chase scenario

V. Acknowledgements

The research presented was funded by Wright-Patterson Air Force Research Laboratory under SFFP .

References

[1] C. Teuliere, L. Eck, and E. Marchand, "Chasing a moving target from a flying UAV," in *Intelligent Robots and Systems (IROS), 2011 IEEE/RSJ International Conference on*. IEEE, 2011, pp. 4929–4934.

[2] T. Oliveira, A. P. Aguiar, and P. Encarnacao, "Moving Path Following for Unmanned Aerial Vehicles With Applications to Single and Multiple Target Tracking Problems," *IEEE Transactions on Robotics*, vol. 32, no. 5, pp. 1062–1078, Oct. 2016. [Online]. Available: http://ieeexplore.ieee.org/document/7553466/

[3] K. B. Ariyur and K. O. Fregene, "Autonomous tracking of a ground vehicle by a UAV," in *American Control Conference, 2008*. IEEE, 2008, pp. 669–671.

[4] J. Lee, R. Huang, A. Vaughn, X. Xiao, J. K. Hedrick, M. Zennaro, and R. Sengupta, "Strategies of path-planning for a UAV to track a ground vehicle," in *AINS Conference*, vol. 2003, 2003.

[5] S. S. Baek, Hyukseong Kwon, J. A. Yoder, and D. Pack, "Optimal path planning of a target-following fixed-wing UAV using sequential decision processes." IEEE, Nov. 2013, pp. 2955–2962. [Online]. Available: http://ieeexplore.ieee.org/document/6696775/

[6] T. Yamasaki, K. Enomoto, H. Takano, Y. Baba, and S. N. Balakrishnan, "Advanced pure pursuit guidance via sliding mode approach for chase UAV," in *Proceedings of AIAA Guidance, Navigation and Control Conference, AIAA*, vol. 6298, 2009, p. 2009.

[7] P. Zarchan and A. Seebass, *Fundamentals of Tactical Missile Guidance*. AIAA Reston, VA, 1994, vol. 157.

[8] N. A. Shneydor, *Missile guidance and pursuit: kinematics, dynamics and control*. Elsevier, 1998.

[9] R. Yanushevsky, *Modern missile guidance*. CRC Press, 2007.

[10] I. E. Weintraub, E. Garcia, D. Casbeer, and M. Pachter, "An optimal aircraft defense strategy for the active target defense scenario."

[11] A. Ratnoo and D. Ghose, "Satisfying terminal angular constraint using proportional navigation," in *Proceeding of AIAA Guidance, Navigation, and Control Conference*, 2009, pp. 1–24.

[12] H. B. Oza and R. Padhi, "Impact-angle-constrained suboptimal model predictive static programming guidance of air-to-ground missiles," *Journal of Guidance, Control and Dynamics*, vol. 35, no. 1, pp. 153–164, 2012.

[13] B.-G. Park, T.-H. Kim, and M.-J. Tahk, "Optimal impact angle control guidance law considering the seeker's field-of-view limits," *Proceedings of the Institution of Mechanical Engineers, Part G: Journal of Aerospace Engineering*, vol. 227, no. 8, pp. 1347–1364, 2013.

[14] S. R. Kumar and D. Ghose, "Three dimensional impact angle constrained guidance law using sliding mode control," in *American Control Conference (ACC), 2014*. IEEE, 2014, pp. 2474–2479.

[15] P. T. Kabamba and A. R. Girard, *Fundamentals of Aerospace navigation and guidance*. Cambridge University Press, 2014.